

SUOD: ACCELERATING LARGE-SCALE UNSUPERVISED HETEROGENEOUS OUTLIER DETECTION

Yue Zhao^{*1} Xiyang Hu^{*1} Cheng Cheng¹ Cong Wang² Changlin Wan³ Wen Wang¹ Jianing Yang¹
Haoping Bai¹ Zheng Li⁴ Cao Xiao⁵ Yunlong Wang⁵ Zhi Qiao⁵ Jimeng Sun⁶ Leman Akoglu¹

ABSTRACT

Outlier detection (OD) is a key data mining task for identifying abnormal objects from general samples with numerous high-stake applications including fraud detection and intrusion detection. Due to the lack of ground truth labels, practitioners often have to build a large number of unsupervised models that are heterogeneous (i.e., different algorithms and hyperparameters) for further combination and analysis with ensemble learning, rather than relying on a single model. However, this yields severe scalability issues on high-dimensional, large datasets.

How to *accelerate* the training and predicting with *a large number of heterogeneous unsupervised OD models*? How to ensure the acceleration does not deteriorate detection models' accuracy? How to accommodate the acceleration need for both a single worker setting and a distributed system with multiple workers? In this study, we propose a three-module acceleration system called SUOD (name anonymized during review) to address these questions. It focuses on three complementary aspects to accelerate (dimensionality reduction for high-dimensional data, model approximation for complex models, and execution efficiency improvement for taskload imbalance within distributed systems), while controlling detection performance degradation. Extensive experiments on more than 20 benchmark datasets demonstrate SUOD's effectiveness in heterogeneous OD acceleration. By the submission time, the released open-source system has been widely used with more than 700,000 times downloads. A real-world deployment case on fraudulent claim analysis at IQVIA, a leading healthcare firm, is also provided.

1 INTRODUCTION

Outlier detection (OD) aims at identifying the samples that are deviant from the general data distribution (Zhao et al., 2019b), which has been used in various applications (Chandola et al., 2009). Notably, most of the existing outlier detection algorithms are unsupervised due to the high cost of acquiring ground truth (Zhao et al., 2019a). However, using a single unsupervised model is risky by nature. Using a large group of unsupervised models with variations are therefore recommended, e.g., different algorithms, varying parameters, distinct views of the datasets, etc (Aggarwal & Sathe, 2017). This is known as heterogeneous OD. Ensemble methods that select and combine diversified base models can be leveraged to analyze heterogeneous OD models (Aggarwal, 2013; Zimek et al., 2014; Aggarwal & Sathe, 2017), and more reliable results may be achieved. The simplest combination is to take the average or maximum across all the base models as the final result (Aggarwal & Sathe,

2017), along with more complex combination approaches in both unsupervised (Zhao et al., 2019a) and semi-supervised manners (Zhao & Hryniewicki, 2018).

However, training and predicting with a large number of heterogeneous OD models can be computationally expensive on high-dimensional, large datasets. For instance, proximity-based algorithms, assuming outliers behave differently in specific regions (Aggarwal, 2016), can be prohibitively slow or even completely fail to work under this setting. For instance, representative methods including k nearest neighbors (k NN) (Ramaswamy et al., 2000), local outlier factor (LOF) (Breunig et al., 2000), and local outlier probabilities (LoOP) (Kriegel et al., 2009), operate in Euclidean space for distance/density calculation, suffering from the curse of dimensionality (Schubert et al., 2015). Numerous works have attempted to tackle this scalability challenge from various angles, e.g., data projection (Keller et al., 2012), subsampling (Liu et al., 2008), and distributed learning for specific OD algorithms (Lozano & Acufia, 2005; Oku et al., 2014). **However, none of them provides a comprehensive solution by considering all aspects of large-scale heterogeneous OD, leading to limited practicability and efficacy.**

To tap the gap, we propose a comprehensive acceleration framework called SUOD (Scalable Unsupervised Outlier

^{*}Equal contribution ¹Carnegie Mellon University ²Peking University ³Purdue University ⁴Arima Inc. ⁵IQVIA ⁶University of Illinois at Urbana-Champaign. Correspondence to: Yue Zhao <zhaoy@cmu.edu>.

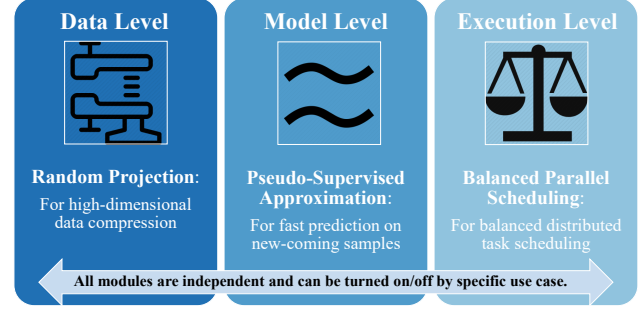
Detection). As shown in Fig. 1, SUOD has three modules focusing on complementary levels: random projection (**data level**), pseudo-supervised approximation (**model level**), and balanced parallel scheduling (**execution level**). For high-dimensional data, SUOD generates a random low-dimensional subspace for each base model by Johnson-Lindenstrauss projection (Johnson & Lindenstrauss, 1984), in which the corresponding base model is trained. If prediction on new-coming samples is needed, fast supervised models are employed to approximate costly unsupervised outlier detectors (that may require pairwise distance calculation). To train the supervised models, we use the unsupervised models’ outputs on the train set as “pseudo ground truth”. Intuitively, this may be viewed as distilling knowledge from slow and complex unsupervised models (Hinton et al., 2015) by fast and more interpretable supervised models. We also propose the first balanced distributed system for heterogeneous OD. Other than generically assign the equal number of models to each worker, our balanced parallel scheduling mechanism can forecast the time cost of each OD model, e.g., training time, before scheduling so that the taskload could be evenly distributed among workers. Notably, all three acceleration modules are designed to be independent but complementary, which can be used alone or combined as a system. It is noted that SUOD is designed for offline learning with a stationary assumption, although it may be extended to online settings for streaming data.

Our contributions are summarized as follows:

1. Examine the impact of various projection methods in OD and identify the performing method(s) for both dimensionality reduction and diversity induction.
2. Analyze pseudo-supervised regression models’ performance in approximating unsupervised OD models. To our best knowledge, this is the first research effort toward leveraging distillation for unsupervised OD.
3. Fix an imbalance scheduling issue in generic, simple distributed systems for heterogeneous OD, with time reduction up to 61%.
4. Conduct extensive experiments to show the effectiveness of the acceleration modules independently, and of the entire framework as a whole, along with a real-world deployment case on claim fraud detection.
5. Open-source the entire system with industry level implementation for accessibility and reproducibility. By the submission time, it has been downloaded by more than 700,000 times with real-world deployment cases¹. It is also integrated as a core component of a leading outlier detection library for large-scale OD.

¹<https://github.com/yzhao062/SUOD>

Figure 1. SUOD focuses on three independent levels.



2 RELATED WORKS

2.1 Outlier Detection and Ensemble Learning

Outlier detection has numerous important applications, such as rare disease detection (Li et al., 2018), healthcare utilization analysis (Hu et al., 2012), video surveillance (Lu et al., 2017), fraudulent online review analysis (Akoglu et al., 2013), and network intrusion detection (Lazarevic et al., 2003). Yet, detecting outliers is challenging due to various reasons (Aggarwal, 2013; Zhao et al., 2019a;b). Most of the existing detection algorithms are unsupervised as ground truth is often absent in practice, and acquiring labels can be prohibitively expensive. Some representative ones used in this study include Isolation Forest (Liu et al., 2008), Local Outlier Factor (LOF) (Breunig et al., 2000), Angle-based Outlier Detection (ABOD) (Kriegel et al., 2009), Feature Bagging (Lazarevic & Kumar, 2005), Histogram-based Outlier Score (HBOS) (Goldstein & Dengel, 2012), and Clustering-Based Local Outlier Factor (CBLOF) (He et al., 2003). See Appendix B for details.

Consequently, relying on a single unsupervised model has inherently high risk, and outlier ensembles that leverage a group of diversified (e.g., heterogeneous) detectors have become increasingly popular (Aggarwal, 2013; Zimek et al., 2014; Aggarwal & Sathe, 2017). There are a group of unsupervised outlier ensemble frameworks proposed in the last several years from simple average, maximization, weighted average, second-phase combination methods (Aggarwal & Sathe, 2017) to more complex selective models like SELECT (Rayana & Akoglu, 2016) and LSCP (Zhao et al., 2019a). Although unsupervised combination can be effective in certain cases, they could not incorporate the existing ground truth information regardless of its richness. As a result, a few semi-supervised detection frameworks that combine existing labels with unsupervised data representation are proposed recently (Micenková et al., 2014; Zhao & Hryniewicki, 2018). For both unsupervised and semi-supervised outlier ensemble methods, a large group of heterogeneous unsupervised OD models are assumed to be used—SUOD is hereby proposed to accommodate the

acceleration need for this scenario.

2.2 Scalability and Efficiency Challenges in OD

Efforts have been made through various channels to accelerate large-scale OD. On the **data level**, researchers try to project high-dimensional data onto lower-dimensional subspaces (Achlioptas, 2001), including simple Principal Component Analysis (PCA) (Shyu et al., 2003) and more complex subspace method HiCS (Keller et al., 2012). However, deterministic projection methods, e.g., PCA, are not ideal for building diversified heterogeneous OD—it leads to the same or similar subspaces with limited diversity by nature, which results in the loss of outliers (Aggarwal, 2016). Complex projection and subspace methods may bring performance improvement for outlier mining, but the generalization capacity is limited. Hence, projection methods preserving pairwise distance relationships for downstream operations should be considered. Beyond preserving pairwise relationship, SUOD’s also considers diversity induction for downstream tasks, leading to both meaningful but diversified feature spaces (see §3.3).

On the **model level**, knowledge distillation emerges as a good way of compressing large neural networks recently (Hinton et al., 2015), while its usage in outlier detection is still underexplored. Knowledge distillation refers to the notion of compressing an ensemble of large, often cumbersome model(s) into a small and more interpretable one(s). A similar idea may be adapted to outlier mining by coupling supervised and unsupervised models. Specifically, proximity-based models, such as LOF, can be slow (high time complexity) for predicting on new-coming samples. Meanwhile, unsupervised OD models generally lack interpretability, which severely restricts their usability in practice. It is noted that SUOD shares a similar concept as knowledge distillation for computational cost optimization but comes with a few fundamental differences (see §3.4).

There are also engineering cures on the **execution level**. For various reasons, OD has no mature and efficient distributed frameworks like Spark—distributed computing for OD mainly falls into the category of “scale-up” that focuses on leveraging multiple local cores on a single machine more efficiently. To this end, specific OD algorithms can be accelerated by distributed computing with multiple workers (e.g., CPU cores) (Lozano & Acufia, 2005; Oku et al., 2014). However, these frameworks are not designed for a group of heterogeneous models but only a single algorithm, which limits their usability. It is noted that a group of heterogeneous detection models can have significantly varied computational cost. As a simple example, let us split 100 heterogeneous models into 4 groups for parallel training. If group #2 takes significantly longer time than the others to finish, it behaves like the bottleneck of the system.

More formally, imbalanced task scheduling leads that the system efficiency is curbed by the worker takes most time. As shown in §3.5, the general distributed task scheduling in machine learning frameworks are inefficient under this setting, which can be improved by SUOD.

3 SYSTEM DESIGN

3.1 Problem Statement

Unsupervised heterogeneous OD training and prediction tasks come with:

- a group of m unsupervised heterogeneous OD models $\mathcal{M} = \{M_1, \dots, M_m\}$. We refer the combination of an algorithm and its corresponding hyperparameters as a model.
- train data $\mathbf{X}_{\text{train}} \in \mathbb{R}^{n \times d}$ without ground truth labels.
- (optional) test data $\mathbf{X}_{\text{test}} \in \mathbb{R}^{l \times d}$ needs prediction with the trained models.
- (optional) t available workers for distributed computing, e.g., t cores on a single machine. This constructs worker pool as $\mathcal{W} = \{W_1, \dots, W_t\}$. By default, a single worker ($t = 1$) is assumed.

Without the SUOD, the general procedure of training models in \mathcal{M} is to train each model M independently on $\mathbf{X}_{\text{train}}$. If there are multiple workers available ($t > 1$), one may equally split m models into t groups, so each available worker is responsible for handling $\frac{m}{t}$ models. Scoring new-coming samples \mathbf{X}_{test} by outlyingness (referred as prediction throughout the paper) follows the similar manner as training.

3.2 The Proposed SUOD System

SUOD is designed to accelerate the above procedures with three independent modules targeting different levels (data, model, and execution). **Each module can be flexibly enabled or disabled** as shown in Algorithm 1. For high-dimensional data, SUOD can randomly projects the original feature onto low-dimensional spaces (§3.3). Pairwise distance relationships are expected to be maintained, and the diversity is induced for ensembling. If prediction on new samples is needed, a fast supervised regressor could be initialized to approximate decision boundary of each costly unsupervised detector so that the original detector can be “retired” during prediction (§3.4). If there are multiple available workers for distributed computing, we propose a balanced scheduling mechanism (§3.5) to expedite the training and prediction execution with a large number of heterogeneous models.

SUOD’s API design is inspired by `scikit-learn` and `PyOD`; it follows an initialization, fit, and prediction schema, as shown in API design demo below.

Algorithm 1 Accelerating large-scale unsupervised heterogeneous outlier detection with SUOD

```

1: Input: a group of  $m$  unsupervised DO models  $\mathcal{M}$ ;
   train data  $\mathbf{X}_{\text{train}} \in \mathbb{R}^{n \times d}$ ; test data  $\mathbf{X}_{\text{test}} \in \mathbb{R}^{l \times d}$  (optional);
   target dimension  $k$ ; pre-trained cost predictor  $C_{\text{cost}}$ ;
   number of available workers  $t$  (default to 1); pre-defined list of costly algorithms  $\mathcal{M}_c$ 
2: Output: fitted (trained) unsupervised models  $\mathcal{M}$ ; fitted pseudo-supervised regressors  $\mathcal{R}$  (optional);
   test prediction results  $\hat{y}_{\text{test}}$  (optional)
3: for each model  $M_i$  in  $\mathcal{M}$  do
4:   if random projection is enabled (§3.3) then
5:     Initialize a JL transformation matrix  $\mathbf{W} \in \mathbb{R}^{d \times k}$ 
6:     Get feature subspace  $\psi_i := \langle \mathbf{X}_{\text{train}}, \mathbf{W} \rangle \in \mathbb{R}^{n \times k}$ 
7:   else
8:     Use the original space  $\psi_i := \mathbf{X}_{\text{train}} \in \mathbb{R}^{n \times d}$ 
9:   end if
10: end for
11: if number of available workers  $t > 1$  then
12:   Split the training of  $m$  models onto  $t$  workers by minimizing Eq. 2 (see §3.5). Each model  $M$  is trained on the processed feature space  $[\psi_1, \dots, \psi_m]$ .
13: else
14:   Train each model  $M_i$  in  $\mathcal{M}$  on its corresponding  $\psi_i$ .
15: end if
16: Return trained models  $\mathcal{M}$ 

```

```

17: if newcoming samples  $\mathbf{X}_{\text{test}}$  needs predicting then
18:   Acquire the pseudo ground truth  $\text{target}^{\psi_i}$  as the output of  $M_i$  on  $\psi_i$ , i.e.,  $\text{target}^{\psi_i} := M_i(\psi_i)$ 
19:   for each costly model  $M_i$  in  $\mathcal{M}_c$  do
20:     Initialize a supervised regressor  $R_i$ 
21:     Fit  $R_i$  by  $\{\psi_i, \text{target}^{\psi_i}\}$  (see §3.4)
22:     Predict by supervised  $R_i$ ,  $\hat{y}_{\text{test}}^i = R_i.\text{predict}(\mathbf{X}_{\text{test}})$ 
23:   end for
24:   Return  $\hat{y}_{\text{test}}$  and approximation regressors  $\mathcal{R}$ 
25: end if

```

3.3 Data Level: Random Projection (RP)

For high-dimensional datasets, many proximity-based OD algorithms suffer from the curse of dimensionality (Lazarevic & Kumar, 2005). A widely used dimensionality reduction to cure this is the Johnson-Lindenstrauss (JL) projection (Johnson & Lindenstrauss, 1984), which has been applied to OD recently because of its great scalability (Schubert et al., 2015). Unlike PCA discussed in §2.2, JL projection could compress the data without heavy distortion on the Euclidean space—outlyingness information is therefore preserved in the compression. Moreover, its built-in randomness can be useful for diversity induction in heterogeneous OD—data randomness can also serve as a source of heterogeneity.

This JL linear transformation is defined as: given a set of

data $\mathbf{X} = \{\mathbf{x}_1, \mathbf{x}_2, \dots, \mathbf{x}_n\}$, each $\mathbf{x}_i \in \mathbb{R}^d$, let \mathbf{W} be a $k \times d$ projection matrix with each entry drawing independently from a predefined distribution like $\mathcal{N}(0, 1)$, where $k < d$. Then the JL projection is a function $f: \mathbb{R}^d \rightarrow \mathbb{R}^k$ such that $f(\mathbf{x}_i) = \frac{1}{\sqrt{k}} \mathbf{x}_i \mathbf{W}^T$. JL projection randomly projects high-dimensional data (d dimensions) to lower-dimensional subspaces (k dimensions), but preserves the distance relationship between points. In fact, if we fix some $\mathbf{v} \in \mathbb{R}^d$, for every $\epsilon \in (0, 3)$, we have (Schubert et al., 2015):

$$P \left[(1 - \epsilon) \|\mathbf{v}\|^2 \leq \left\| \frac{1}{\sqrt{k}} \mathbf{v} \mathbf{W}^T \right\|^2 \leq (1 + \epsilon) \|\mathbf{v}\|^2 \right] \leq 2e^{-\epsilon^2 \frac{k}{6}} \quad (1)$$

Let \mathbf{v} to be the differences between vectors. Then, the above bound shows that for a finite set of N vectors $\mathbf{X} = \{\mathbf{x}_1, \mathbf{x}_2, \dots, \mathbf{x}_n\} \in \mathbb{R}^d$, the pairwise Euclidean distance is preserved within a factor of $(1 \pm \epsilon)$, given reducing the vectors to $k = \mathcal{O}(\frac{\log(N)}{\epsilon^2})$ dimensions.

Four JL projection variants are considered in this study: (i) *basic*: the transformation matrix is generated by standard Gaussian; (ii) *discrete*: the transformation matrix is picked randomly from Rademacher distribution (uniform in $\{-1, 1\}$); (iii) *circulant*: the transformation matrix is obtained by rotating the subsequent rows from the first row which is generated from standard Gaussian and (iv) *toeplitz*: the first row and column of the transformation matrix are generated from standard Gaussian, and each diagonal uses a constant value from the first row and column. A more thorough empirical study on JL methods can be found in (Venkatasubramanian & Wang, 2011).

For $\mathbf{X}_{\text{train}}$ with d features, the projection module can be invoked to reduce the original feature space to the target dimension k . That is, SUOD can use a JL transformation matrix $\mathbf{W} \in \mathbb{R}^{d \times k}$ initialized by one of the JL projection methods, to efficiently project $\mathbf{X}_{\text{train}}$ onto the k dimension feature space, $\mathbf{X}'_{\text{train}} = \langle \mathbf{X}_{\text{train}}, \mathbf{W} \rangle \in \mathbb{R}^{n \times k}$. The transformation matrix \mathbf{W} is also kept for prediction: $\mathbf{X}'_{\text{test}} = \langle \mathbf{X}_{\text{test}}, \mathbf{W} \rangle \in \mathbb{R}^{m \times k}$. Nonetheless, RP module should be used with caution. First, projection may be less useful or even detrimental for subspace methods like Isolation Forest and HBOS. Second, if the number of samples n is too small, the above JL bound does not hold.

3.4 Model Level: Pseudo-Supervised Approximation (PSA)

For the case that prediction on new-coming samples is needed, PSA module can be leveraged to speed up model prediction. Once a model M in \mathcal{M} is trained, SUOD can approximate and replace each **costly unsupervised model** by a **faster supervised regressor for predicting outlyingness scores on new-coming samples in an offline fashion**. It is worth mentioning that not all unsupervised models

. SUOD API design follows scikit-learn style and is easy to use

```
import SUOD
# initialize a group of OD models
>>> base_estimators = [
    LOF(n_neighbors=40),
    ABOD(n_neighbors=50),
    LOF(n_neighbors=60),
    IForest(n_estimators=100)]
# initialize SUOD with module flags
>>> clf =
    SUOD(base_estimators=base_estimators,
        rp_flag_global=True,
        approx_clf=approx_clf,
        bps_flag=True,
        approx_flag_global=True)
# fit and make prediction
>>> clf.fit(X_train)
>>> y_test_labels = clf.predict(X_test)
>>> y_test_scores =
    clf.decision_function(X_test)
```

need replacing but only the costly ones. The cost can be measured through time complexity of prediction. For instance, proximity based algorithms like k NN and LOF are costly in prediction (upper bounded by $\mathcal{O}(nd)$), and can be effectively replaced by fast supervised models like random forest (Breiman, 2001) (upper bounded by $\mathcal{O}(ph)$ where p denotes the number of base trees and h denotes the max depth of a tree; often $p \ll n$ and $h \leq d$). This “pseudo-supervised” model uses the output of unsupervised models (outlyingness score) as “the pseudo ground truth”—the goal is to approximate the decision boundaries of the underlying unsupervised model. The chosen approximator’s prediction cost should be lower than the underlying unsupervised model, while maintaining a comparable level of accuracy on new-coming samples. Consequently, fast OD algorithms like Isolation Forest and HBOS with low time complexity should not be approximated and replaced. To facilitate this process, we create a list of costly OD algorithm pool \mathcal{M}_c . If a model M_i falls in the algorithm category of \mathcal{M}_c , it will be approximated by default.

As shown in Algorithm 1, for each trained unsupervised model M_i for i in $\{1, \dots, m\}$, a supervised regressor R_i might be trained by $\{\mathbf{X}_{\text{train}}, \mathbf{y}_i\}$; \mathbf{y}_i is the outlyingness score by M_i on the train set (referred as pseudo ground truth). R_i is then used to predict on unseen data \mathbf{X}_{test} .

Remark 1: Supervised ensemble-based tree models are recommended for model approximation due to their outstanding scalability, robustness to overfitting, and interpretability (e.g., feature importance) (Hu et al., 2019). In addition to the execution time reduction, supervised models generally show better interpretability compared with unsupervised counterparts. For instance, random forest used in the ex-

periments can yield feature importance automatically to facilitate understanding.

Remark 2: Notably, PSA may be viewed as using supervised regressors to distill knowledge from unsupervised OD models. However, it works in a fully unsupervised manner, unlike the classic distillation under supervised settings.

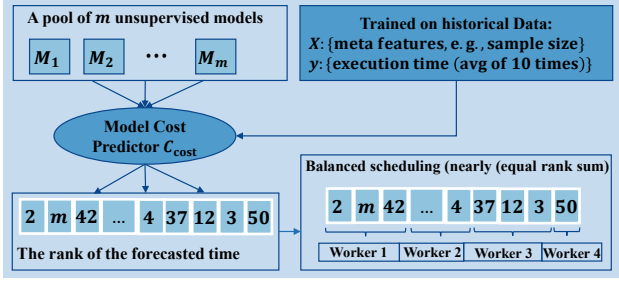
3.5 Execution level: Balanced Parallel Scheduling (BPS)

Taskload Imbalance within Distributed Systems: if there are multiple workers available for distributed computing, BPS can assign tasks more evenly across all available workers by forecasting model cost, for both training and prediction stage. *Without the forecast model, practitioners often use generic scheduling by distributing equal number of models to each worker.* It is noted taskload imbalance among workers curbs an efficient execution. For instance, one may train 25 OD models with varying parameters from each of the four algorithm groups $\{k$ NN, Isolation Forest, HBOS, OCSVM $\}$, resulting in 100 models in total. The existing distributed frameworks, e.g., the voting machine in scikit-learn (Pedregosa et al., 2011) or general frameworks like joblib¹, will simply split the models into 4 subgroups by order and schedule the first 25 models (all k NNs) on worker 1, the next 25 models on worker 2, etc. This does not account for the fact that within a group of heterogeneous models, the computational cost varies. Scheduling the task with the equal number of models can result in highly imbalanced load. In the worst-case scenario, one worker may be assigned significant more load than the rest, resulting in halt to the entire process. In this example, the k NN subgroup will be the system curb due to high time complexity. Obviously, this problem applies to both training and prediction stage. One solution is to shuffle the base models randomly. However, there is no guarantee this heuristic could work, and it may be practically infeasible.

The proposed BPS heuristic focuses on delivering a more balanced task schedule among workers. Ideally, all workers can finish the scheduled tasks within a similar duration and return the results. To achieve this goal, SUOD comes with a *model cost predictor* C_{cost} to forecast the model execution time (sum of 10 trials) given the meta-features (descriptive features) of a dataset (Zhao et al., 2020), including input data size, input data dimension, the algorithm embedding, etc. The *model cost predictor* is trained on 11 algorithm family with 47 benchmark datasets by 10-fold cross validation, yielding a performing regressor (random forest is used in this study). The trained C_{cost} can predict the rank of the running time with high accuracy; its Spearman’s Rank correlation (Spearman, 1904) to the true model cost rank is consistently high ($r_s > 0.9$) with low

¹<https://github.com/joblib/joblib>

Figure 2. Flowchart of balanced parallel scheduling, which aims to assign nearly equal rank sum by model cost predictor C_{cost} .



p-value ($p < 0.0001$), in all folds.

As a result, a scheduling heuristic is proposed by enforcing a nearly equal rank sum by forecasted execution time, as shown in Fig. 2. Given m models to be trained (or used for prediction), cost predictor C_{cost} is first invoked to forecast the execution time for each model M in \mathcal{M} as $C_{\text{cost}}(M)$ and output the model cost rank of each model in $\{1, m\}$. If there are t cores (workers), each worker will be assigned a group of models to achieve the objective of minimizing the taskload imbalance among workers (Eq. 2). Consequently, each worker is assigned with a group of models with the rank sum close to the average rank sum $\frac{(1+m)m}{2} / t = \frac{m^2+m}{2t}$. Indeed, the accurate running time prediction is less relevant as it depends on the hardware—the rank is more useful as a relevance measure with the transferability to other hardware. That is, the running time will vary on different machines, but the relative rank should preserve. One issue around the sum of ranks is the overestimation of high-rank models. For instance, rank f -th model will be counted f times more heavily than rank 1 model during the sum calculation, even their actual running time difference will not be as big as f times. To fix this, we introduce a discounted rank by rescaling model rank f to $1 + \frac{\alpha f}{m}$, where α denotes the scaling strength (default to 1).

$$\min_{\mathcal{W}} \sum_{i=1}^t \left| \sum_{M_j \in \mathcal{W}_i} C_{\text{cost}}(\mathcal{D}_i) - \frac{m^2+m}{2t} \right| \quad (2)$$

It is noted that building multiple large neural networks is rare in outlier detection due to computational consideration. Therefore, the model cost predictor only covers the major methods in Python Outlier Detection Toolbox (PyOD) (Zhao et al., 2019b). For unseen models, they are classified as “unknown” to be assigned with the max cost to prevent overoptimistic scheduling.

4 NUMERICAL EXPERIMENTS & DISCUSSION

First, three experiments are conducted to understand the effectiveness of individual modules independently: **Q1**: how will different projection methods affect the performance of downstream OD accuracy (§4.1); **Q2**: will pseudo-supervised regressors lead to degraded prediction performance compared to the original unsupervised models (§4.2) and **Q3**: under which conditions (number of models m , number of workers t , etc.), will the proposed balanced scheduling outperform the baseline (§4.3). Then, the full SUOD with all three modules enabled is evaluated regarding time cost and prediction accuracy (on new samples) (§4.4). Finally, a real-world deployment case on fraudulent claim analysis at IQVIA, one of the global leading healthcare organizations, is described (§4.5). The details of OD models and datasets used in this study can be found in the Appendix.

4.1 Q1: The Comparison of Projection Methods

To evaluate the effect of data projection, we choose three costly outlier detection algorithms namely, ABOD, LOF, and k NN to measure their execution time, and prediction accuracy (ROC and P@N), before and after projection. These methods directly or indirectly measure sample similarity in Euclidean space, e.g., pairwise distance, which is prone to the curse of dimensionality and projection may be helpful.

Table 1 shows the comparison results on three datasets; the reduced dimension is set as $k = \frac{2}{3}d$. We compare the proposed four JL projection methods (see §3.3 for details of *basic*, *discrete*, *circulant*, and *toeplitz*) with **original** (no projection), **PCA**, and **RS** (randomly select k features from the original d features, used in Feature Bagging (Lazarevic & Kumar, 2005) and LSCP (Zhao et al., 2019a)). First, all projection methods show superiority regarding time cost. Second, using **original** method shows high instability—it rarely performs the best, which is consistent with the findings in literature (Zhao et al., 2019a). Third, **PCA** is inferior to **original** regarding prediction accuracy (see LOF performance in Table 1e, 1f, and 1g). The observation supports our claim that PCA is not suited in this scenario (see §2.2). Fourth, JL methods generally lead to equivalent or better prediction performance than **original** regarding both time and prediction accuracy. Lastly, among all four JL methods, *circulant* and *toeplitz* outperform others in most cases, and are recommended as default projection methods in SUOD.

4.2 Q2: The Visual and Quantitative Analysis of PSA

To better understand the effect of PSA, we first generate 200 synthetic two-dimensional points with Normal distribution for outliers (40 points) and Uniform distribution for

Table 1. Comparison of various projection methods on different outlier detectors and datasets. Each column corresponds to an evaluation metric (execution time is measured in seconds); the best performing method is indicated in **bold**. JL projection methods, especially *circulant* and *toeplitz*, outperform regarding both time cost and prediction accuracy.

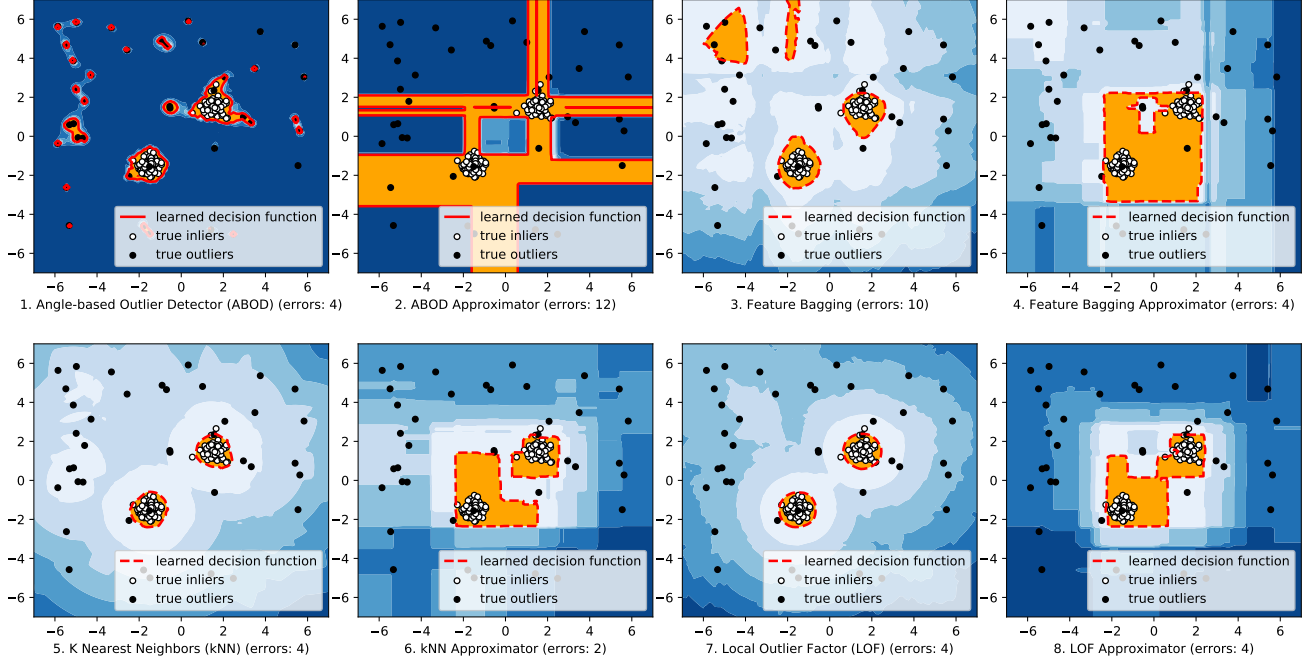
(a) ABOD on MNIST				(b) ABOD on Satellite				(c) ABOD on Satimage-2			
Method	Time	ROC	P@N	Method	Time	ROC	P@N	Method	Time	ROC	P@N
original	12.89	0.80	0.39	original	4.03	0.59	0.41	original	3.68	0.85	0.28
PCA	8.93	0.81	0.37	PCA	3.01	0.62	0.44	PCA	2.70	0.88	0.30
RS	8.27	0.74	0.32	RS	3.53	0.63	0.44	RS	3.20	0.89	0.28
<i>basic</i>	8.94	0.80	0.38	<i>basic</i>	3.10	0.64	0.45	<i>basic</i>	2.78	0.91	0.29
<i>discrete</i>	8.86	0.80	0.39	<i>discrete</i>	3.12	0.65	0.46	<i>discrete</i>	2.79	0.91	0.31
<i>circulant</i>	9.33	0.80	0.38	<i>circulant</i>	3.14	0.66	0.48	<i>circulant</i>	2.85	0.91	0.29
<i>toeplitz</i>	8.96	0.80	0.38	<i>toeplitz</i>	3.14	0.66	0.47	<i>toeplitz</i>	2.83	0.92	0.30
(d) ABOD on Cardio				(e) LOF on MNIST				(f) LOF on Satellite			
Method	Time	ROC	P@N	Method	Time	ROC	P@N	Method	Time	ROC	P@N
original	0.98	0.59	0.25	original	7.64	0.68	0.29	original	0.82	0.55	0.37
PCA	0.82	0.59	0.26	PCA	4.92	0.67	0.27	PCA	0.23	0.54	0.36
RS	0.92	0.63	0.29	RS	3.65	0.63	0.23	RS	0.39	0.54	0.37
<i>basic</i>	0.83	0.62	0.28	<i>basic</i>	4.87	0.70	0.31	<i>basic</i>	0.31	0.54	0.37
<i>discrete</i>	0.82	0.62	0.28	<i>discrete</i>	5.21	0.70	0.32	<i>discrete</i>	0.32	0.54	0.37
<i>circulant</i>	0.83	0.62	0.27	<i>circulant</i>	5.06	0.69	0.31	<i>circulant</i>	0.39	0.55	0.38
<i>toeplitz</i>	0.83	0.62	0.28	<i>toeplitz</i>	4.97	0.71	0.31	<i>toeplitz</i>	0.37	0.54	0.37
(g) LOF on Satimage-2				(h) LOF on Cardio				(i) kNN on MNIST			
Method	Time	ROC	P@N	Method	Time	ROC	P@N	Method	Time	ROC	P@N
original	0.79	0.54	0.07	original	0.08	0.55	0.17	original	7.13	0.84	0.42
PCA	0.20	0.52	0.04	PCA	0.04	0.56	0.19	PCA	3.92	0.84	0.40
RS	0.37	0.53	0.08	RS	0.04	0.57	0.15	RS	3.33	0.77	0.34
<i>basic</i>	0.29	0.52	0.08	<i>basic</i>	0.04	0.60	0.20	<i>basic</i>	4.17	0.84	0.42
<i>discrete</i>	0.30	0.53	0.07	<i>discrete</i>	0.04	0.59	0.19	<i>discrete</i>	4.11	0.84	0.41
<i>circulant</i>	0.43	0.59	0.11	<i>circulant</i>	0.04	0.59	0.20	<i>circulant</i>	4.13	0.84	0.41
<i>toeplitz</i>	0.32	0.54	0.09	<i>toeplitz</i>	0.04	0.60	0.21	<i>toeplitz</i>	4.11	0.84	0.42
(j) kNN on Satellite				(k) kNN on Satimage-2				(l) kNN on Cardio			
Method	Time	ROC	P@N	Method	Time	ROC	P@N	Method	Time	ROC	P@N
original	0.71	0.67	0.49	original	0.68	0.94	0.39	original	0.09	0.71	0.34
PCA	0.18	0.67	0.50	PCA	0.15	0.94	0.39	PCA	0.03	0.73	0.34
RS	0.31	0.68	0.49	RS	0.29	0.94	0.38	RS	0.03	0.69	0.38
<i>basic</i>	0.24	0.68	0.49	<i>basic</i>	0.23	0.94	0.38	<i>basic</i>	0.03	0.74	0.35
<i>discrete</i>	0.25	0.69	0.50	<i>discrete</i>	0.20	0.95	0.37	<i>discrete</i>	0.03	0.74	0.37
<i>circulant</i>	0.33	0.70	0.50	<i>circulant</i>	0.36	0.96	0.37	<i>circulant</i>	0.03	0.74	0.34
<i>toeplitz</i>	0.30	0.70	0.51	<i>toeplitz</i>	0.25	0.96	0.39	<i>toeplitz</i>	0.03	0.73	0.35

normal samples (160 points). In Fig. 3, we plot the decision surfaces of unsupervised models and their corresponding supervised approximators (random forest regressor). In general, the pseudo supervised approximators show equal or lower errors, suggesting the suitability of approximation (lower errors on Feature Bagging and k NN as shown in Fig. 3 subfigure 4 and 6). We notice that the decision surfaces of the approximators are different and some regularization effect appears. One assumption is that the approximation process improves the generalization ability of the model

by “ignoring” the overfitted points. This fails to work with ABOD because it has an extremely coarse decision surface to approximate (Fig. 3, subfigure 1).

Table 2 and Appendix Table C.1 compare prediction performance (scoring on new-coming samples) between the original unsupervised models and pseudo-supervised approximators on 10 datasets with 6 costly algorithms. These algorithms are more computationally expensive than random forest regressors for prediction. The prediction time comparison is omitted due to space limit, but the gain is

Figure 3. Decision surface comparison among unsupervised models and their pseudo-supervised counterparts (in pairs). The approximator’s decision boundary shows a tentative regularization effect over the original ones, which leads to lower or no worse errors.



clear. Therefore, the focus is whether the approximators could predict unseen samples as good as the original unsupervised models. The tables reveal that not all the algorithms can be approximated well by supervised regressors: ABOD has a performance decrease regarding ROC on multiple datasets. Notably, ABOD is a linear model that look for a low-dimensional subspace to embed the normal samples (Aggarwal, 2016), so the approximation may not work if it has extremely complex decision surfaces as mentioned before. In contrast, proximity-based models benefit from the approximation. Both table show, k NN, LoF, and ak NN (average k NN) experience a performance gain. Specifically, all three algorithms yield around 100% ROC increase on **HTTP**. Other algorithms, such as Feature Bagging and CBLOF, the ROC and PRC performances stay within the acceptable range. In other words, it is useful to perform pseudo-supervised approximation for these estimators as the time efficiency is improved at little to no loss in prediction accuracy. Through both visualization and quantitative comparisons, we believe that the proposed PSA is meaningful for offline prediction acceleration.

4.3 Q3: The Time Reduction Effect of Balanced Scheduling

To evaluate the effectiveness of the proposed BPS algorithm, we run the following experiments by varying: (i) the size (n) and the dimension (d) of the datasets, (ii) the number of estimators (m) and (iii) the number of CPU cores (t). Due to

the space limit, we only show the training time comparison between the generic scheduling and BPS on **Cardio**, **Letter**, **PageBlock**, and **Pendigits**, by setting $m \in \{100, 500\}$ and $t \in \{2, 4, 8\}$, which is consistent with the single machine used in real-world applications.

Table 3 shows that the proposed BPS has a clear edge over the generic scheduling mechanism (denoted as **Generic** in the tables) that equally splits the tasks by order. It yields a significant time reduction (denoted as **% Redu** in the table), and gets more remarkable if more cores are used along with large datasets. For instance, the time reduction is more than 40% on **PageBlock** and **Pendigits** when 8 cores are used. This agrees with our assumption as model cost should vary more drastically on large datasets if the time complexity is not linear—the proposed BPS method is particularly helpful.

4.4 SUOD: Full System Evaluation

Table 4 shows the performance of SUOD with all three modules enabled, even not all of them are always needed in practice. In total, 600 hundred random OD models from **PyOD** are trained and tested on 10 datasets. To simulate the “worst-case scenario” performance of the framework, the model order is randomized to minimize the intrinsic task load imbalance. In real-world applications, this order randomization may not be possible as discussed in §3.5. **Although this setting reduces the significance of time reduction of the BPS module, we choose it to provide an empirical worst-case performance guarantee—the framework**

Table 2. Prediction ROC scores of unsupervised models (Orig) and their pseudo-supervised approximators (Appr) by the average of 10 independent trials. The better method within each pair is indicated in **bold**. The approximators (Appr) outperform in most cases.

Dataset	Anthyroid		Breastw		Cardio		HTTP		MNIST		Pendigits		Pima		Satellite		Satimage-2		Thyroid	
Model	Orig	Appr	Orig	Appr	Orig	Appr	Orig	Appr	Orig	Appr	Orig	Appr	Orig	Appr	Orig	Appr	Orig	Appr	Orig	Appr
ABOD	0.83	0.71	0.92	0.93	0.63	0.53	0.15	0.13	0.81	0.79	0.67	0.82	0.66	0.70	0.59	0.68	0.89	0.99	0.96	0.67
CBLOF	0.67	0.68	0.96	0.98	0.73	0.76	1.00	1.00	0.85	0.89	0.93	0.93	0.63	0.68	0.72	0.77	1.00	1.00	0.92	0.97
FB	0.81	0.45	0.34	0.10	0.61	0.70	0.34	0.97	0.72	0.83	0.39	0.51	0.59	0.63	0.53	0.64	0.36	0.40	0.83	0.46
kNN	0.80	0.79	0.97	0.97	0.73	0.75	0.19	0.85	0.85	0.86	0.74	0.87	0.69	0.71	0.68	0.75	0.96	0.99	0.97	0.98
akNN	0.81	0.82	0.97	0.97	0.67	0.72	0.19	0.88	0.84	0.85	0.72	0.87	0.69	0.71	0.66	0.74	0.95	0.99	0.97	0.98
LOF	0.74	0.85	0.44	0.45	0.60	0.68	0.35	0.75	0.72	0.76	0.38	0.47	0.59	0.65	0.53	0.66	0.36	0.38	0.80	0.95

 Table 3. Training time comparison (in seconds) between Simple scheduling and BPS against various number of OD models and workers. Percent of time reduction, Redu (%), is indicated in **bold**. BPS consistently outperform to Generic scheduling

Dataset	<i>n</i>	<i>d</i>	<i>m</i>	<i>t</i>	Generic	BPS	Redu (%)
Cardio	1831	21	500	2	240.12	221.34	7.82
Cardio	1831	21	500	4	185.44	154.43	16.72
Cardio	1831	21	500	8	140.63	120.02	14.65
Cardio	1831	21	1000	2	199.77	185.63	7.08
Cardio	1831	21	1000	4	130.82	110.60	15.45
Cardio	1831	21	1000	8	97.75	73.43	24.88
Letter	1600	32	500	2	111.95	109.52	2.17
Letter	1600	32	500	4	92.69	86.24	6.94
Letter	1600	32	500	8	57.21	48.72	14.84
Letter	1600	32	1000	2	224.61	222.59	0.90
Letter	1600	32	1000	4	228.08	172.07	24.56
Letter	1600	32	1000	8	109.50	89.51	17.80
PageBlock	5393	10	100	2	51.11	35.17	31.19
PageBlock	5393	10	100	4	42.49	16.23	61.80
PageBlock	5393	10	100	8	38.45	16.97	55.86
PageBlock	5393	10	500	2	197.84	137.46	30.52
PageBlock	5393	10	500	4	167.36	76.14	54.51
PageBlock	5393	10	500	8	127.08	66.29	47.84
Pendigits	6870	16	500	2	351.97	287.14	18.42
Pendigits	6870	16	500	4	288.51	146.50	49.22
Pendigits	6870	16	500	8	180.86	102.11	43.33
Pendigits	6870	16	1000	2	697.20	561.15	19.51
Pendigits	6870	16	1000	4	579.70	288.11	50.33
Pendigits	6870	16	1000	8	365.20	182.32	50.08

should surely perform better in practice.

SUOD consistently yields promising results even we deliberately choose the unfavor setting. **Fit_B** and **Pred_B** denote the fit and prediction time of the baseline setting (no projection, no approximation, generic parallel task scheduling; see §2.2). In comparison, SUOD (denoted as **Fit_S** and **Pred_S**) brings time reduction on majority of the datasets with minor to no performance degradation. To measure the prediction performance, we measure the ROC and P@N by averaging the base model results (denoted as **Avg₋**) and the maximum of average of the base models (denoted as **MOA₋**), a widely used two-phase outlier score combination framework (Aggarwal & Sathe, 2017). Surprisingly, SUOD even leads to small performance boost in scoring new samples on most of the datasets (**Anthyroid**, **Cardio**, **MNIST**, **Optdigits**, **Pendigits**, and **Thyroid**). This performance gain may be jointly credited to the regularization effect by the randomness injected in JL projection

(§3.3) and the pseudo-approximation (§3.4)—the baseline setting may be overfitted on certain datasets. It is noted that SUOD leads to more improvement on high-dimensional, large datasets. For instance, the fit time is significantly reduced on **Shuttle**. On the contrary, SUOD is less useful for small datasets like **Pima** and **Cardio**, although they may also yield performance improvement. Again, our settings mimics the worst case scenario for SUOD (the model order is already randomly shuffled) but still observe a great performance improvement; real-world applications should generally expect more significant results.

4.5 Real-World Deployment: Fraudulent Medical Claim Analysis at IQVIA

Estimated by the United States Government Accountability Office and Federal Bureau of Investigation, healthcare frauds cost American taxpayers tens of billions dollars a year (Bagdoyan, 2018; Aldrich et al., 2014). Detecting fraudulent medical claims is crucial for taxpayers, pharmaceutical companies and insurance companies. To further demonstrate SUOD’s performance on industry data, we deploy it on a proprietary pharmacy claim dataset owned by IQVIA, a leading healthcare firm, consisting of 123,720 medical claims among which 19,033 (15.38%) are labeled as fraudulent. In each of the claim, there are 35 features including information such as drug brand, copay amount, insurance details, location and pharmacy/patient demographics. The current system in use is based on a group of selected detection models in PyOD, and an averaging method is applied on top of the base model results as the initial result. The cases marked as high risk are then transferred to human investigators in special investigation unit (SIU) for verification. It is important to provide prompt and accurate first-round screening for SIU, which leads to huge expense save.

SUOD is applied on top of the aforementioned dataset (74,220 records are used for training and 49,500 records are set aside for validation). Similarly to the full framework evaluation in §4.4, the new system with SUOD (all three modules enabled) is compared with the current distributed system on 10 cores. The fit time is reduced from 6232.54 seconds to 4202.30 seconds (32.57% reduction), and the prediction time is reduced from 3723.45 seconds reduced to

Table 4. Comparison between the baseline (denoted as .B) and SUOD (denoted as .S) regarding time cost, and prediction accuracy (ROC and P@N). The better method within each pair is indicated in **bold** (Optdigits fail to yield meaningful P@N). SUOD generally brings time reduction with no loss in prediction accuracy on majority of datasets.

Data Information				Time Cost (in seconds)				Ensemble Model Performance (ROC)				Ensemble Model Performance (P@N)			
Dataset	<i>n</i>	<i>d</i>	<i>t</i>	Fit.B	Fit.S	Pred.B	Pred.S	Avg.B	Avg.S	MOA.B	MOA.S	Avg.B	Avg.S	MOA.B	MOA.S
Anthyroid	7200	6	5	73.91	65.23	47.48	44.26	0.91	0.93	0.91	0.93	0.46	0.54	0.46	0.55
Anthyroid	7200	6	10	71.00	42.94	44.68	38.66	0.91	0.93	0.92	0.93	0.46	0.54	0.46	0.54
Anthyroid	7200	6	30	42.80	33.98	30.92	25.67	0.91	0.93	0.92	0.93	0.46	0.54	0.46	0.54
Cardio	1831	21	5	78.84	79.70	46.09	46.68	0.91	0.93	0.91	0.93	0.46	0.54	0.45	0.55
Cardio	1831	21	10	72.04	53.43	44.57	38.31	0.91	0.93	0.91	0.93	0.46	0.54	0.46	0.54
Cardio	1831	21	30	47.53	44.57	31.31	31.43	0.91	0.93	0.92	0.93	0.46	0.54	0.46	0.55
MNIST	7603	100	5	856.53	748.40	453.39	324.76	0.77	0.81	0.77	0.81	0.29	0.35	0.28	0.34
MNIST	7603	100	10	726.76	573.66	367.85	328.95	0.78	0.81	0.78	0.81	0.29	0.35	0.30	0.34
MNIST	7603	100	30	357.40	329.71	260.80	134.08	0.78	0.81	0.78	0.81	0.29	0.35	0.29	0.34
Optdigits	5216	64	5	295.38	267.71	162.28	149.19	0.73	0.75	0.75	0.77	0.00	0.00	0.00	0.00
Optdigits	5216	64	10	247.24	224.82	136.12	125.54	0.73	0.75	0.74	0.75	0.00	0.00	0.00	0.00
Optdigits	5216	64	30	825.23	791.95	110.06	62.63	0.73	0.75	0.73	0.76	0.00	0.00	0.00	0.00
Pendigits	6870	16	5	287.75	282.25	184.20	158.26	0.92	0.95	0.92	0.94	0.19	0.23	0.19	0.20
Pendigits	6870	16	10	281.49	155.06	179.83	160.94	0.92	0.95	0.92	0.94	0.19	0.25	0.19	0.23
Pendigits	6870	16	30	149.93	145.59	104.25	89.85	0.92	0.94	0.93	0.94	0.19	0.25	0.19	0.22
Pima	768	8	5	28.72	31.94	21.16	23.79	0.71	0.71	0.71	0.70	0.51	0.51	0.53	0.51
Pima	768	8	10	27.38	20.15	20.81	25.03	0.71	0.70	0.71	0.70	0.51	0.51	0.51	0.51
Pima	768	8	30	19.36	17.89	13.83	17.43	0.71	0.70	0.71	0.70	0.51	0.50	0.52	0.50
Shuttle	49097	9	5	3326.54	1453.93	2257.50	1956.12	0.99	0.99	0.99	0.99	0.95	0.95	0.95	0.95
Shuttle	49097	9	10	2437.10	1396.21	1549.97	1321.16	0.99	0.99	0.99	0.99	0.95	0.95	0.95	0.95
Shuttle	49097	9	30	1378.29	1258.69	837.41	651.00	0.99	0.99	0.99	0.99	0.95	0.95	0.95	0.95
SpamSpace	4207	57	5	247.98	244.39	130.95	110.08	0.57	0.56	0.56	0.56	0.45	0.45	0.46	0.45
SpamSpace	4207	57	10	233.39	186.91	128.24	115.83	0.57	0.56	0.56	0.56	0.46	0.45	0.46	0.46
SpamSpace	4207	57	30	604.00	538.91	70.19	61.38	0.57	0.56	0.57	0.56	0.46	0.46	0.46	0.45
Thyroid	3772	6	5	87.90	71.34	49.51	48.20	0.91	0.93	0.91	0.93	0.46	0.54	0.46	0.55
Thyroid	3772	6	10	74.76	46.91	44.81	38.60	0.91	0.93	0.91	0.93	0.46	0.54	0.46	0.54
Thyroid	3772	6	30	45.84	43.86	28.90	26.75	0.91	0.93	0.92	0.93	0.46	0.54	0.46	0.54
Waveform	3443	21	5	167.98	147.00	109.94	94.46	0.78	0.76	0.78	0.76	0.11	0.13	0.11	0.13
Waveform	3443	21	10	154.72	94.36	91.69	55.17	0.78	0.76	0.78	0.77	0.11	0.11	0.11	0.11
Waveform	3443	21	30	97.11	95.77	53.47	48.04	0.78	0.76	0.78	0.76	0.11	0.13	0.11	0.13

2814.92 seconds (24.40%). In addition to the time reduction, ROC and P@N also shows an improvement at 3.59% and 7.46%, respectively. Through this case, we are confident the proposed framework can be useful for many real-world applications for scalable learning.

5 CONCLUSION & FUTURE DIRECTIONS

In this work, a three-module acceleration SUOD is proposed to expedite the training and prediction with a large number of unsupervised heterogeneous outlier detection models. The three modules in SUOD focus on different levels (data, model, execution): (i) Random Projection module generates low-dimensional subspaces to alleviate the curse of dimensionality using Johnson-Lindenstrauss projection; (ii) Pseudo-supervised Approximation module could accelerate costly unsupervised models' prediction by replacing them by cheaper supervised regressors, which also brings the extra benefit regarding interpretability and (iii) Balanced Parallel Scheduling module ensures that nearly equal amount of workload is assigned to multiple workers in distributed computing. The extensive experiments on more than 20 benchmark datasets and a real-world claim fraud analysis case show the great potential of SUOD, and many intriguing results are observed. For reproducibility and ac-

cessibility, all code, figures, and datasets are openly shared¹. By the submission time, the SUOD has been widely used by practitioners with more than 700,000 downloads.

Many investigations are underway. First, we plan to demonstrate SUOD's effectiveness as an end-to-end framework on more complex downstream combination models like unsupervised LSCP (Zhao et al., 2019a) and supervised XG-BOD (Zhao & Hryniewicki, 2018). Second, we would further emphasize the interpretability provided by the pseudo-supervised approximation, which can be beyond simple feature importance provided in tree regressors. Third, we see there is room to investigate why and how the pseudo-supervised approximation could work in a more strict and theoretical way. This study, as the first step, empirically shows that proximity-based models benefit from the approximation. Fourth, other classical acceleration methods may be explored as well, e.g., giving attention to numeric precision optimization (Rusci et al., 2020). Lastly, we may incorporate the emerging automated outlier detection, e.g., MetaOD (Zhao et al., 2020), to trim down the model space for further acceleration.

¹<https://github.com/yzhao062/SUOD>

REFERENCES

- Achlioptas, D. Database-friendly random projections. In *PODS*. ACM, 2001.
- Aggarwal, C. C. Outlier ensembles: position paper. *ACM SIGKDD Explorations Newsletter*, 14(2):49–58, 2013.
- Aggarwal, C. C. *Outlier Analysis*. Springer, 2016.
- Aggarwal, C. C. and Sathe, S. *Outlier ensembles: An introduction*. Springer, 1st edition, 2017. ISBN 9783319547657.
- Akoglu, L., Chandy, R., and Faloutsos, C. Opinion fraud detection in online reviews by network effects. In *ICWSM*, 2013.
- Aldrich, N., Crowder, J., and Benson, B. How much does medicare lose due to fraud and improper payments each year. *The Sentinel*, 2014.
- Bagdoyan, S. J. Medicare: Actions needed to better manage fraud risks. <https://www.gao.gov/assets/700/693156.pdf>, 2018.
- Breiman, L. Random forests. *Machine learning*, 45(1): 5–32, 2001.
- Breunig, M. M., Kriegel, H.-P., Ng, R. T., and Sander, J. LOF: Identifying Density-Based Local Outliers. *SIGMOD*, pp. 1–12, 2000. ISSN 01635808.
- Chandola, V., Banerjee, A., and Kumar, V. Anomaly detection: A survey. *CSUR*, 41(3):15, 2009.
- Goldstein, M. and Dengel, A. Histogram-based outlier score (hbos): A fast unsupervised anomaly detection algorithm. *KI-2012: Poster and Demo Track*, pp. 59–63, 2012.
- He, Z., Xu, X., and Deng, S. Discovering cluster-based local outliers. *Pattern Recognition Letters*, 24(9-10):1641–1650, 2003.
- Hinton, G., Vinyals, O., and Dean, J. Distilling the knowledge in a neural network. *arXiv preprint arXiv:1503.02531*, 2015.
- Hu, J., Wang, F., Sun, J., Sorrentino, R., and Ebadollahi, S. A healthcare utilization analysis framework for hot spotting and contextual anomaly detection. In *AMIA annual symposium proceedings*, 2012.
- Hu, X., Rudin, C., and Seltzer, M. Optimal sparse decision trees. *NeurIPS*, pp. 7265–7273, 2019.
- Johnson, W. B. and Lindenstrauss, J. Extensions of lipschitz mappings into a hilbert space. *Contemporary mathematics*, 26(189-206):1, 1984.
- Keller, F., Muller, E., and Bohm, K. Hics: High contrast subspaces for density-based outlier ranking. In *ICDE*, 2012.
- Kriegel, H.-P., Schubert, M., and Zimek, A. Angle-based outlier detection in high-dimensional data. In *KDD*, pp. 444–452. ACM, 2008.
- Kriegel, H.-P., Kröger, P., Schubert, E., and Zimek, A. LoOP: local outlier probabilities. *CIKM*, pp. 1649–1652, 2009.
- Lazarevic, A. and Kumar, V. Feature bagging for outlier detection. In *KDD*, pp. 157–166. ACM, 2005.
- Lazarevic, A., Ertoz, L., Kumar, V., Ozgur, A., and Srivastava, J. A comparative study of anomaly detection schemes in network intrusion detection. In *SDM*, pp. 25–36, 2003.
- Li, W., Wang, Y., Cai, Y., Arnold, C., Zhao, E., and Yuan, Y. Semi-supervised rare disease detection using generative adversarial network. In *NeurIPS Workshop*, 2018.
- Liu, F. T., Ting, K. M., and Zhou, Z.-H. Isolation forest. In *ICDM*, 2008.
- Liu, Y., Li, Z., Zhou, C., Jiang, Y., Sun, J., Wang, M., and He, X. Generative adversarial active learning for unsupervised outlier detection. *TKDE*, 2019.
- Lozano, E. and Acufia, E. Parallel algorithms for distance-based and density-based outliers. In *ICDM*, 2005.
- Lu, W., Cheng, Y., Xiao, C., Chang, S., Huang, S., Liang, B., and Huang, T. Unsupervised sequential outlier detection with deep architectures. *IEEE Transactions on Image Processing*, 26(9):4321–4330, 2017.
- Micenkova, B., McWilliams, B., and Assent, I. Learning outlier ensembles: The best of both worlds—supervised and unsupervised. In *SIGKDD Workshop*, pp. 51–54, 2014.
- Oku, J., Tamura, K., and Kitakami, H. Parallel processing for distance-based outlier detection on a multi-core cpu. In *IEEE International Workshop on Computational Intelligence and Applications (IWCIA)*, pp. 65–70. IEEE, 2014.
- Pedregosa, F., Varoquaux, G., Gramfort, A., Michel, V., Thirion, B., Grisel, O., Blondel, M., Prettenhofer, P., Weiss, R., et al. Scikit-learn: Machine learning in python. *JMLR*, 2011.
- Ramaswamy, S., Rastogi, R., Shim, K., Hill, M., Shim, K., and Ramaswamy, Sridhar, Rajeev rastogi, K. S. Efficient algorithms for mining outliers from large data sets. *ACM SIGMOD Record*, 29(2):427–438, 2000. ISSN 01635808.

- Rayana, S. and Akoglu, L. Less is more: Building selective anomaly ensembles. *TKDD*, 10(4):42, 2016.
- Rusci, M., Capotondi, A., and Benini, L. Memory-driven mixed low precision quantization for enabling deep network inference on microcontrollers. In Dhillon, I., Papailiopoulos, D., and Sze, V. (eds.), *Proceedings of Machine Learning and Systems*, volume 2, pp. 326–335. 2020.
- Schölkopf, B., Platt, J. C., Shawe-Taylor, J., Smola, A. J., and Williamson, R. C. Estimating the support of a high-dimensional distribution. *Neural computation*, 2001.
- Schubert, E., Zimek, A., and Kriegel, H.-P. Fast and scalable outlier detection with approximate nearest neighbor ensembles. In *DASFAA*, 2015.
- Shyu, M.-L., Chen, S.-C., Sarinnapakorn, K., and Chang, L. A novel anomaly detection scheme based on principal component classifier. Technical report, 2003.
- Spearman, C. The proof and measurement of association between two things. *AJP*, 1904.
- Venkatasubramanian, S. and Wang, Q. The johnson-lindenstrauss transform: an empirical study. In *ALLENEX Workshop*, pp. 164–173. SIAM, 2011.
- Zhao, Y. and Hryniewicki, M. K. Xgbod: Improving supervised outlier detection with unsupervised representation learning. In *IJCNN*. IEEE, 2018.
- Zhao, Y., Nasrullah, Z., Hryniewicki, M. K., and Li, Z. LSCP: locally selective combination in parallel outlier ensembles. In *SDM*, pp. 585–593, 2019a.
- Zhao, Y., Nasrullah, Z., and Li, Z. PyOD: A python toolbox for scalable outlier detection. *JMLR*, 20(96):1–7, 2019b.
- Zhao, Y., Rossi, R. A., and Akoglu, L. Automating outlier detection via meta-learning. *arXiv preprint arXiv:2009.10606*, 2020.
- Zimek, A., Campello, R. J., and Sander, J. Ensembles for unsupervised outlier detection: challenges and research questions a position paper. *ACM SIGKDD Explorations Newsletter*, 15(1):11–22, 2014.

SUPPLEMENTARY MATERIAL

Details on Datasets, Models, and Additional Results.

A DATASETS AND SETUP

Table A.1 describes the selected outlier detection benchmark datasets, and more than 20 outlier detection benchmark datasets are used in this study^{1,2}. The data size n varies from 452 (**Arrhythmia**) to 567,479 (**HTTP**) samples and the dimension d ranges from 3 to 274. For both random projection and parallel scheduling experiments, the full datasets are used for model building (training). For the pseudo-supervised approximation experiments and the full framework assessment, 60% of the data is used for training and the remaining 40% is set aside for validation. For all experiments, performance is evaluated by taking the average of 10 independent trials using area under the receiver operating characteristic (ROC) curve and precision at rank n (P@N)—here n denotes the actual number of outliers. Both metrics are widely used in outlier research (Zimek et al., 2014; Liu et al., 2019).

Table A.1. Selected real-world benchmark datasets

Dataset	Pts (n)	Dim (d)	Outliers	% Outlier
Anthyroid	7200	6	534	7.41
Arrhythmia	452	274	66	14.60
Breastw	683	9	239	34.99
Cardio	1831	21	176	9.61
HTTP	567479	3	2211	0.40
Letter	1600	32	100	6.25
MNIST	7603	100	700	9.21
Musk	3062	166	97	3.17
PageBlock	5393	10	510	9.46
Pendigits	6870	16	156	2.27
Pima	768	8	268	34.90
Satellite	6435	36	2036	31.64
Satimage-2	5803	36	71	1.22
seismic	2584	10	170	6.59
Shuttle	49097	9	3511	7.15
SpameSpace	4207	57	1679	39.91
speech	3686	400	61	1.65
Thyroid	3772	6	93	2.47
Vertebral	240	6	30	12.50
Vowels	1456	12	50	3.43
Waveform	3443	21	100	2.90
Wilt	4819	5	257	5.33

B OUTLIER DETECTION MODELS

As shown in Table B.1, we use a large group of outlier detection models in the experiment by varying algorithms and their corresponding hyperparameters.

¹ODDS Library: <http://odds.cs.stonybrook.edu>

²DAMI Datasets: <http://www.dbs.ifi.lmu.de/research/outlier-evaluation/DAMI>

C ADDITIONAL EXPERIMENT RESULTS

Here we present the additional comparison result of prediction performance between the original unsupervised models and pseudo-supervised approximators on 10 datasets with 6 costly algorithms by P@N (see §4.2). The approximators outperform in most cases.

Table B.1. Outlier Detection Models in SUOD; see parameter definitions from PyOD (Zhao et al., 2019b)

Method	Parameter 1	Parameter 2
ABOD (Kriegel et al., 2008)	n_neighbors: [3, 5, 10, 15, 20, 25, 50, 60, 70, 80, 90, 100]	N/A
CBLOF (He et al., 2003)	n_clusters: [3, 5, 10, 15, 20]	N/A
Feature Bagging (Lazarevic & Kumar, 2005)	n_estimators: [10, 20, 30, 40, 50, 75, 100, 150, 200]	N/A
HBOS (Goldstein & Dengel, 2012)	n_histograms: [5, 10, 20, 30, 40, 50, 75, 100]	tolerance: [0.1, 0.2, 0.3, 0.4, 0.5]
iForest (Liu et al., 2008)	n_estimators: [10, 20, 30, 40, 50, 75, 100, 150, 200]	max_features: [0.1, 0.2, 0.3, 0.4, 0.5, 0.6, 0.7, 0.8, 0.9]
kNN (Ramaswamy et al., 2000)	n_neighbors: [1, 5, 10, 15, 20, 25, 50, 60, 70, 80, 90, 100]	method: ['largest', 'mean', 'median']
LOF (Breunig et al., 2000)	n_neighbors: [1, 5, 10, 15, 20, 25, 50, 60, 70, 80, 90, 100]	method: ['manhattan', 'euclidean', 'minkowski']
OCSVM (Schölkopf et al., 2001)	nu (train error tol): [0.1, 0.2, 0.3, 0.4, 0.5, 0.6, 0.7, 0.8, 0.9]	kernel: ['linear', 'poly', 'rbf', 'sigmoid']

Table C.1. Prediction P@N scores of unsupervised models (Orig) and their pseudo-supervised approximators (Appr) by the average of 10 independent trials. The better method within each pair is indicated in **bold**. The approximators (Appr) outperform in most cases.

Dataset	Annnthyroid		Breastw		Cardio		HTTP		MNIST		Pendigits		Pima		Satellite		Satimage-2		Thyroid	
Model	Orig	Appr	Orig	Appr	Orig	Appr	Orig	Appr	Orig	Appr	Orig	Appr	Orig	Appr	Orig	Appr	Orig	Appr	Orig	Appr
ABOD	0.31	0.08	0.80	0.83	0.27	0.20	0.00	0.00	0.40	0.27	0.05	0.05	0.48	0.52	0.41	0.46	0.21	0.64	0.36	0.00
CBLOF	0.25	0.24	0.86	0.90	0.31	0.34	0.02	0.01	0.42	0.48	0.35	0.36	0.43	0.48	0.54	0.57	0.96	0.96	0.26	0.38
FB	0.24	0.02	0.03	0.07	0.23	0.26	0.02	0.04	0.34	0.36	0.03	0.07	0.37	0.44	0.37	0.42	0.03	0.04	0.05	0.02
kNN	0.30	0.32	0.89	0.89	0.37	0.46	0.03	0.03	0.42	0.45	0.08	0.06	0.47	0.47	0.49	0.53	0.32	0.43	0.33	0.42
AkNN	0.30	0.33	0.88	0.89	0.34	0.40	0.03	0.03	0.41	0.45	0.05	0.13	0.48	0.49	0.47	0.52	0.25	0.43	0.31	0.44
LOF	0.27	0.36	0.19	0.35	0.23	0.23	0.01	0.03	0.33	0.32	0.03	0.08	0.40	0.44	0.37	0.42	0.04	0.07	0.19	0.25